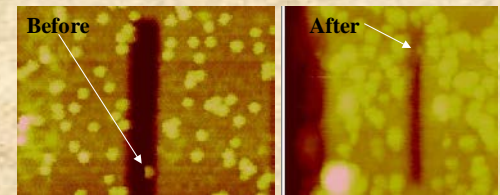
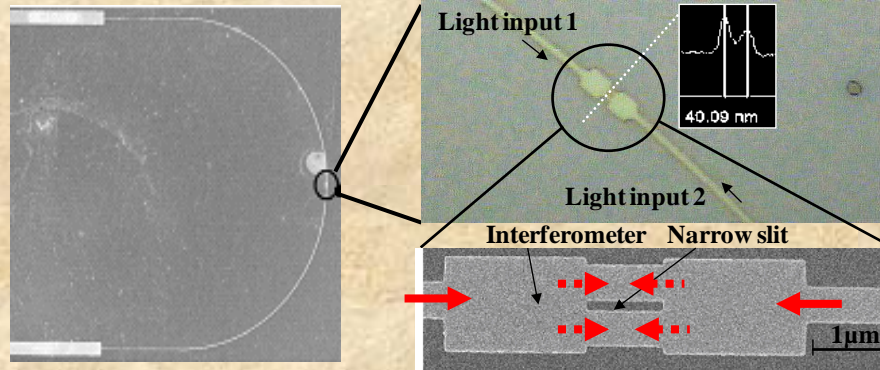
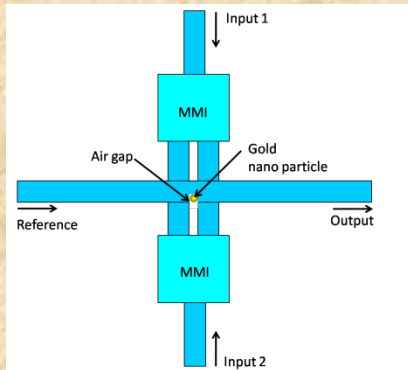


Novel Concepts for Photonic Ranging

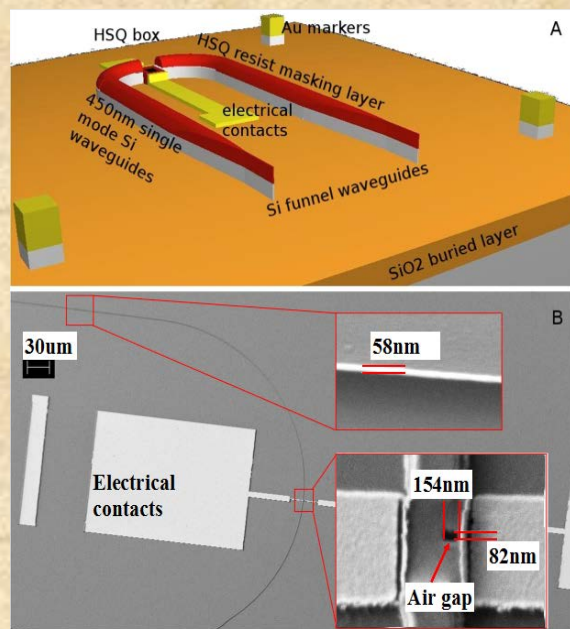
Zeev Zalevsky

**Faculty of Engineering, Bar-Ilan University, 52900
Ramat-Gan, Israel**

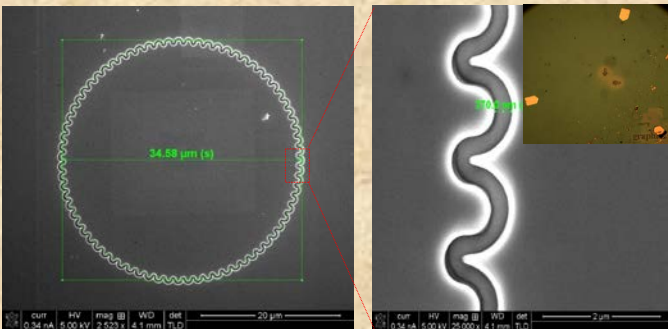
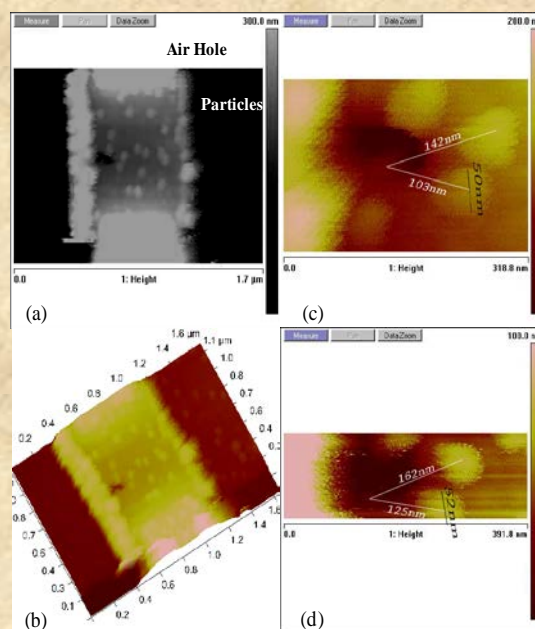


Shifting particle along the slit with only 100nW!
(coupled power)

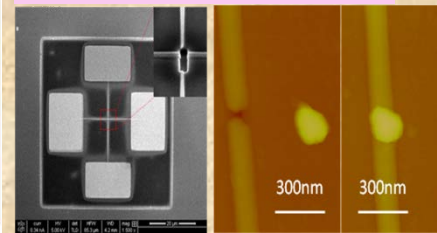
Trapped nano particle: all-optical modulator, sensor, wavelength converter, logic gate and flip flop



Particle based electro-optical modulator



Tunable nano source



Electronic nano transistor

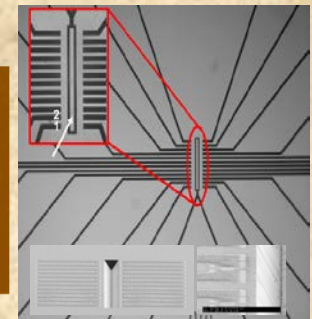
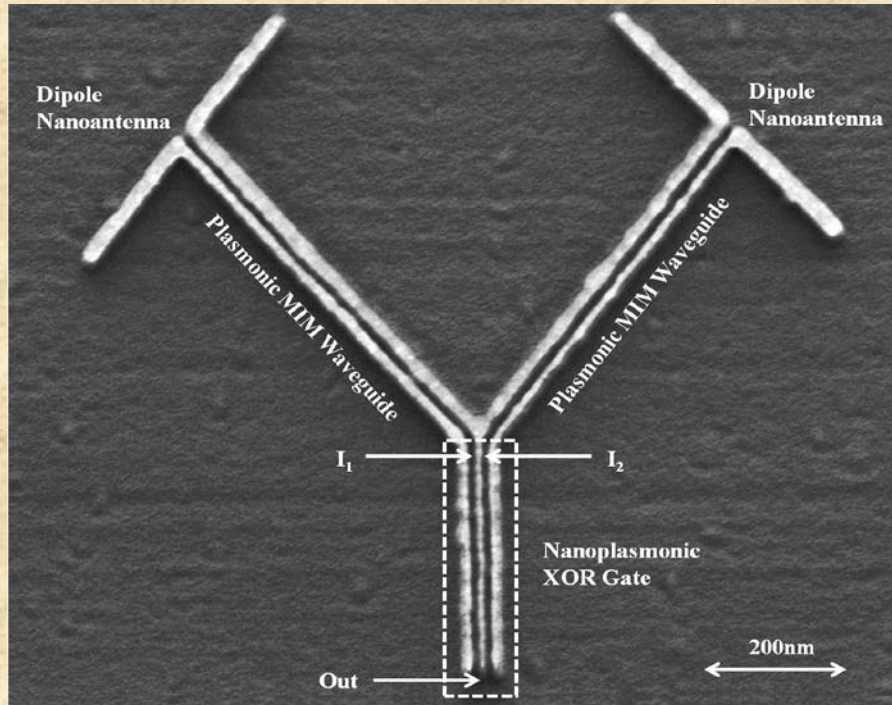


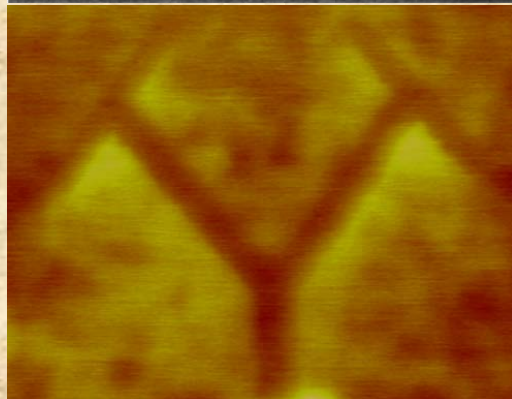
Photo-initiated transistor



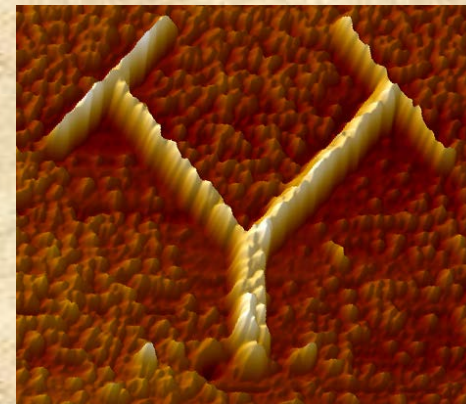
High resolution microscopy image of the fabricated plasmonic structure.

The silver structures are shown in bright colors, and the gray background represents the SOI substrate.

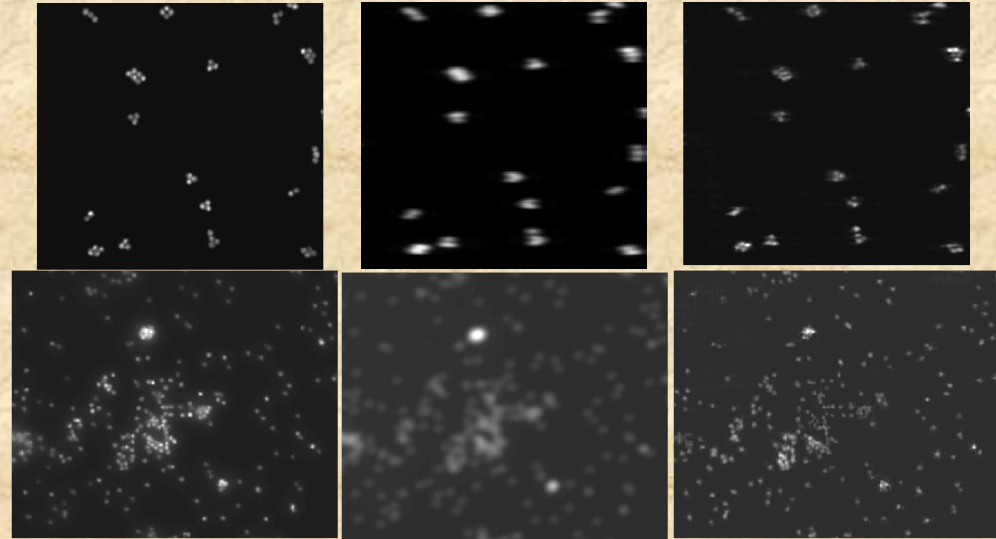
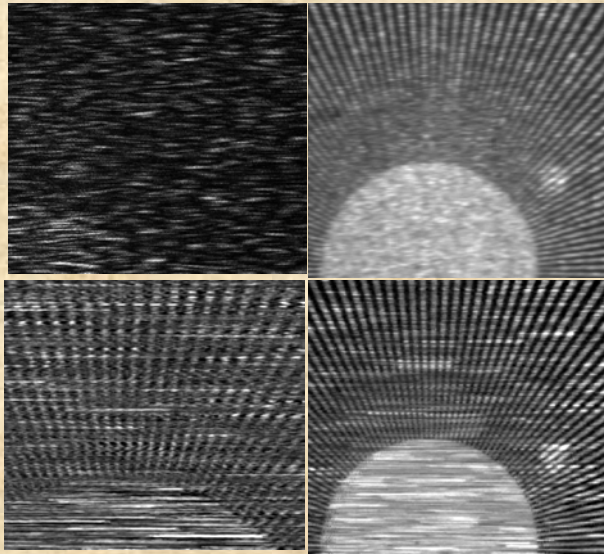
Performances characterization of the nanoplasmonic logic XOR gate, integrated with the excitation and waveguiding system



Two dimensional measurement of surface electric potential on the fabricated plasmonic structure, obtained by the AFM system. Both nanoantennas are illuminated.



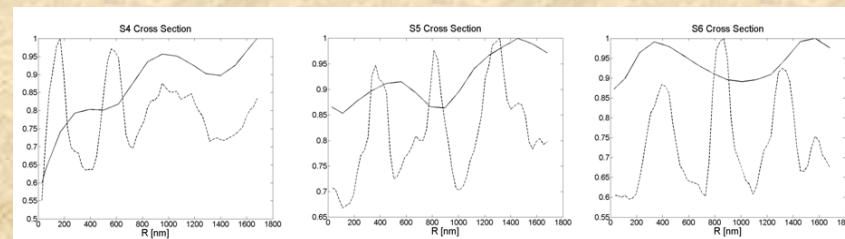
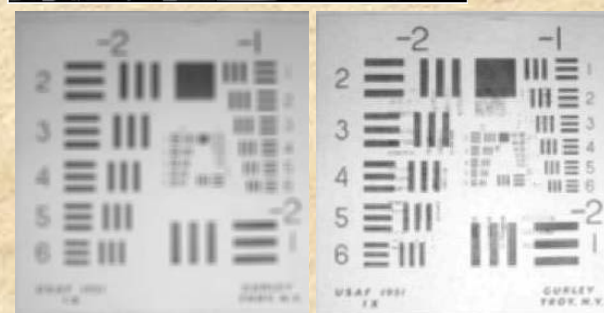
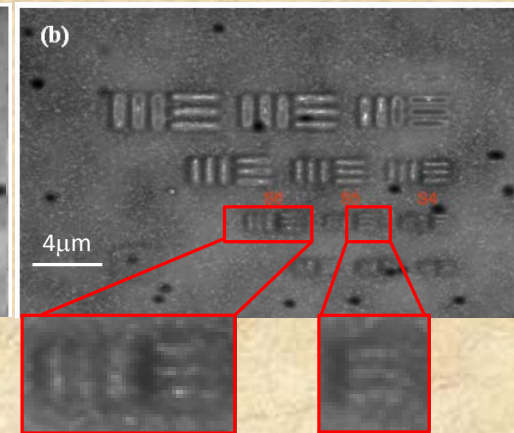
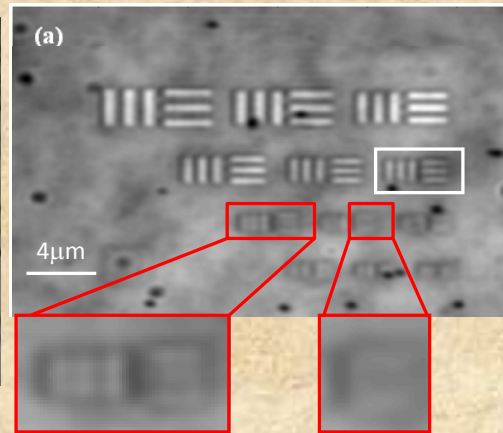
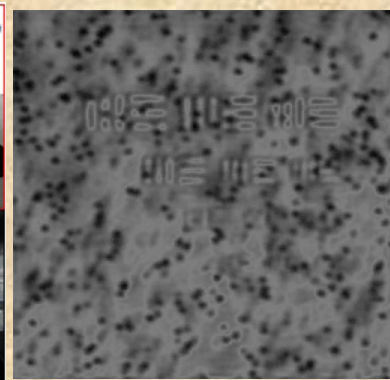
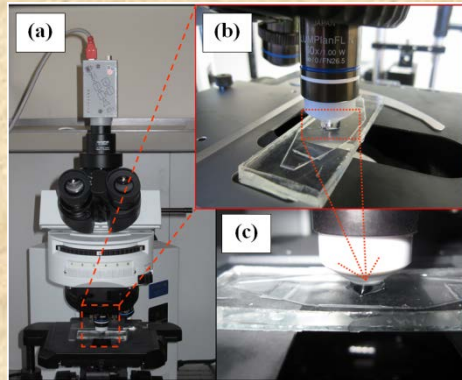
3D image of the fabricated nanoplasmonic system, created by high resolution AFM microscope.



Open aperture

Closed aperture

Reconstruction



Main collaborators:

Hamootal Duadi¹

Javier Garcia²

Eyal Gordon³

Gur Arie Bittan³

Amihai Loven³

¹Faculty of Engineering, Bar-Ilan University, Israel

²Departamento de Óptica, Universitat de València, Spain

³Mantis Vision

Outline

- Introduction
- Review of new approaches
- Correlation based 3D estimation
- Conclusions

Outline

- Introduction
- Review of new approaches
- Correlation based 3D estimation
- Conclusions

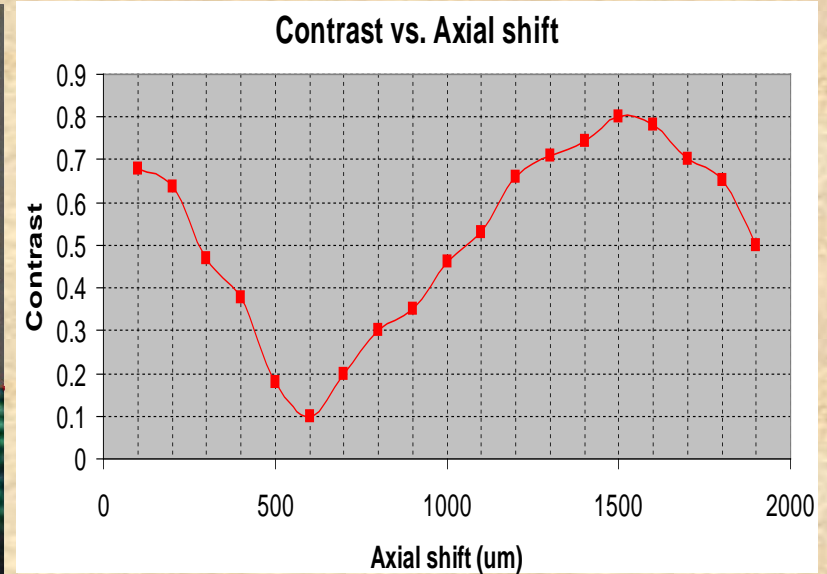
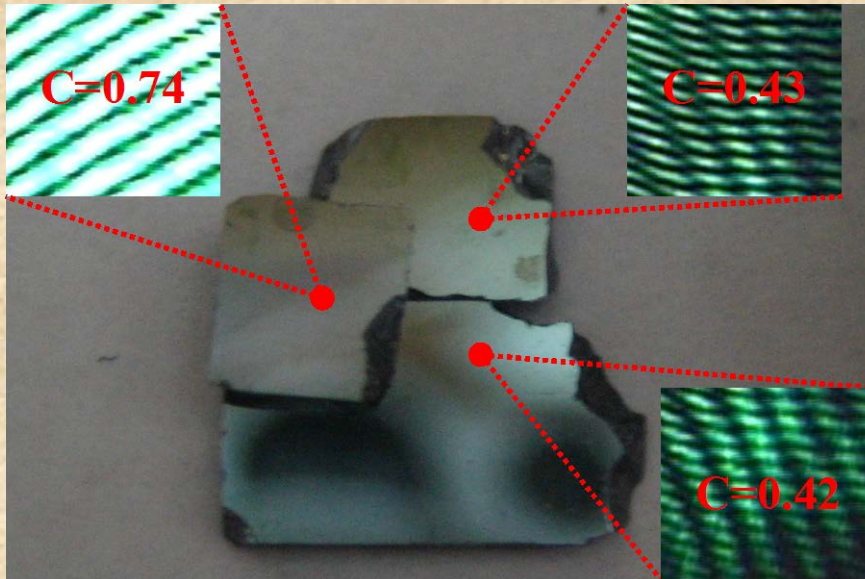
Techniques for ranging/3D estimation

- Stereoscopy with 2 cameras
- Holography (e.g. digital)
- Coherence (temporal e.g. OCT and spatial)
- Image processing
 - Range from defocus
 - Range from shading
 - Geometrical projections/transformations
- LIDAR
- Patterns projection
 - Phase shift
 - Scanning line
 - Random pattern projection (speckles)
 - Z varied pattern

Outline

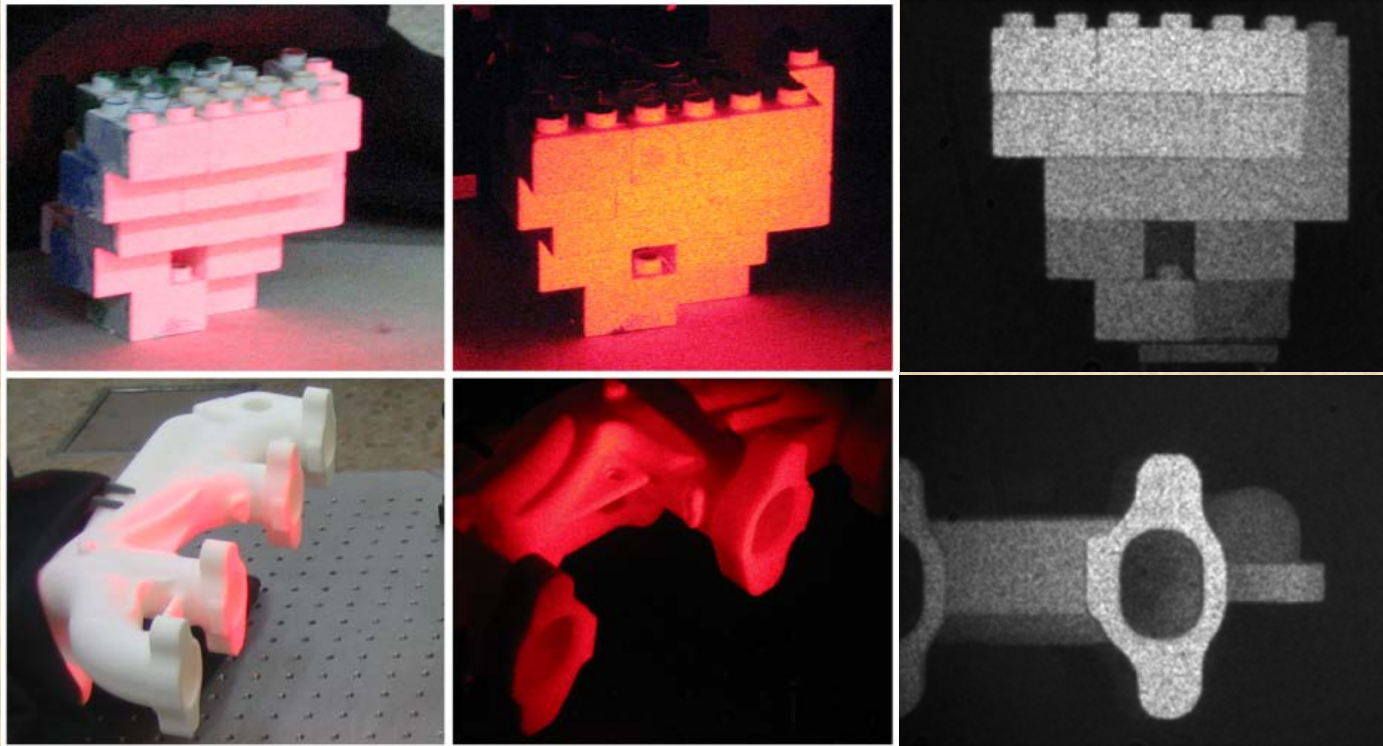
- Introduction
- Review of new approaches
- Correlation based 3D estimation
- Conclusions

Temporal coherence

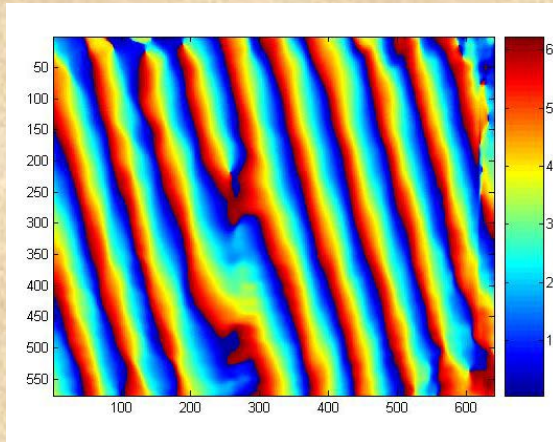


3D estimation by computing localized interference fringes contrast. (a). The measured contrast. (b). Calibration reference curve.

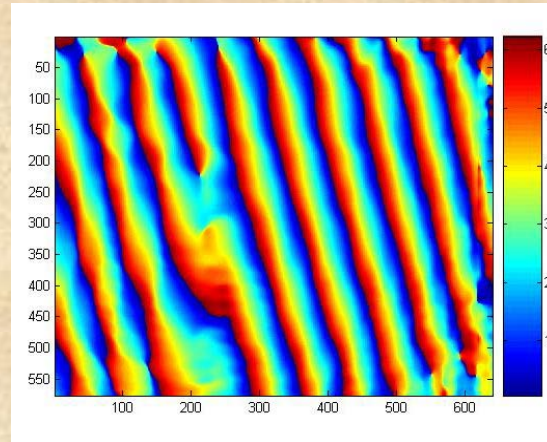
Coherence mapping- Speckles



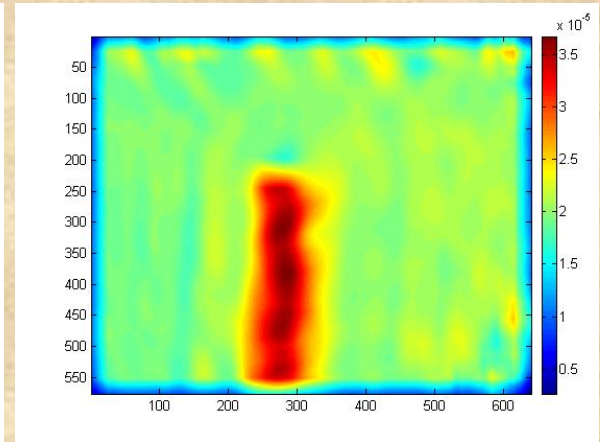
An electronic speckle pattern interferometric (ESPI) setup, where the object depth is encoded into the amplitude of the interference pattern. After performing phase-shifting method, the object's 3-D shape is reconstructed by means as a range image from the visibility of the image set of interferograms and where each gray level is representative of a given object depth.



(a).

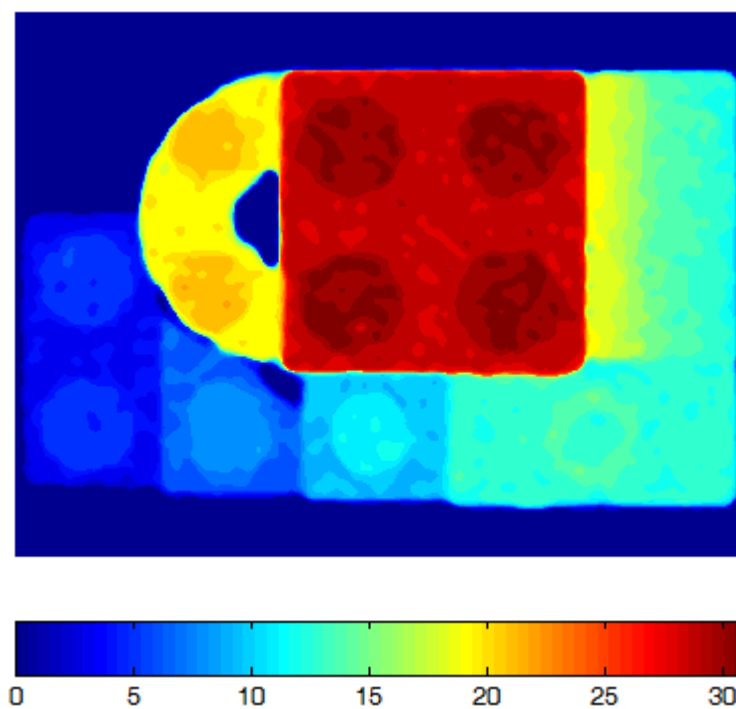
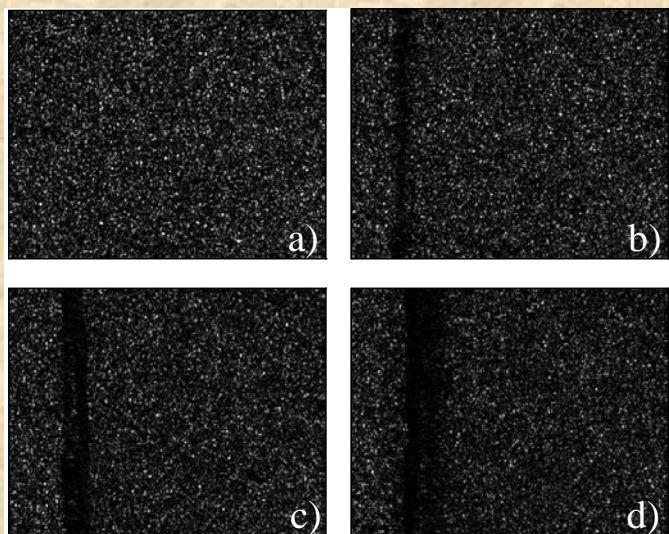
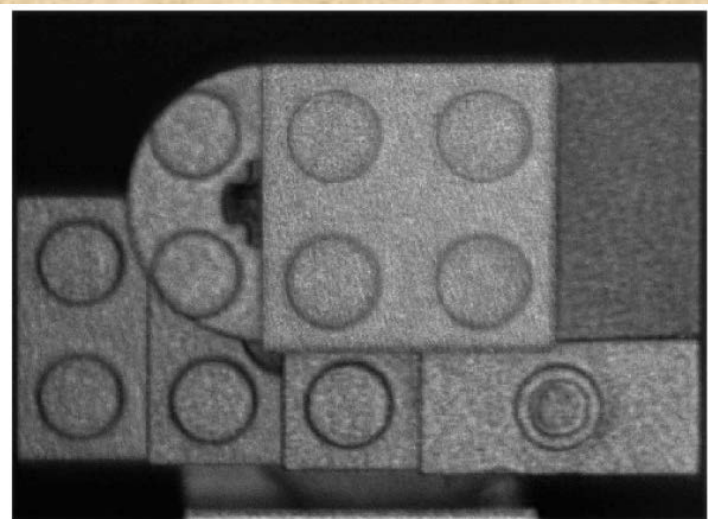


(b).

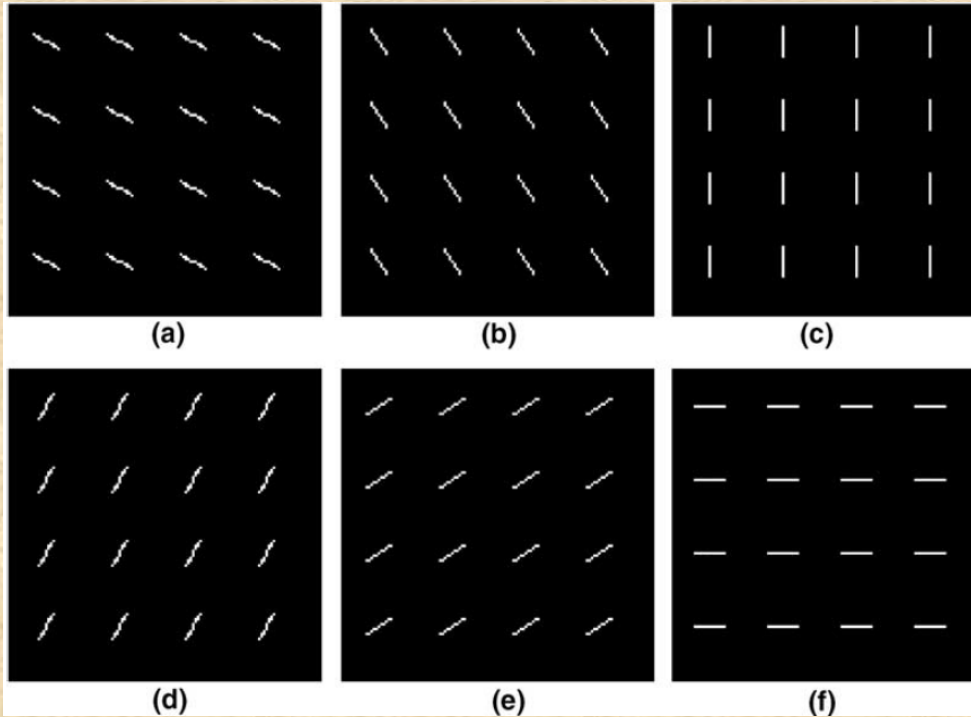


Phase unwrapping. (a). Phase reconstruction for two angles projection which were separated by 1 degree. (b). The profile reconstruction. Each pixel is the pixel of the camera which was $6.7\mu\text{m}$. The alleviation width is in meters.

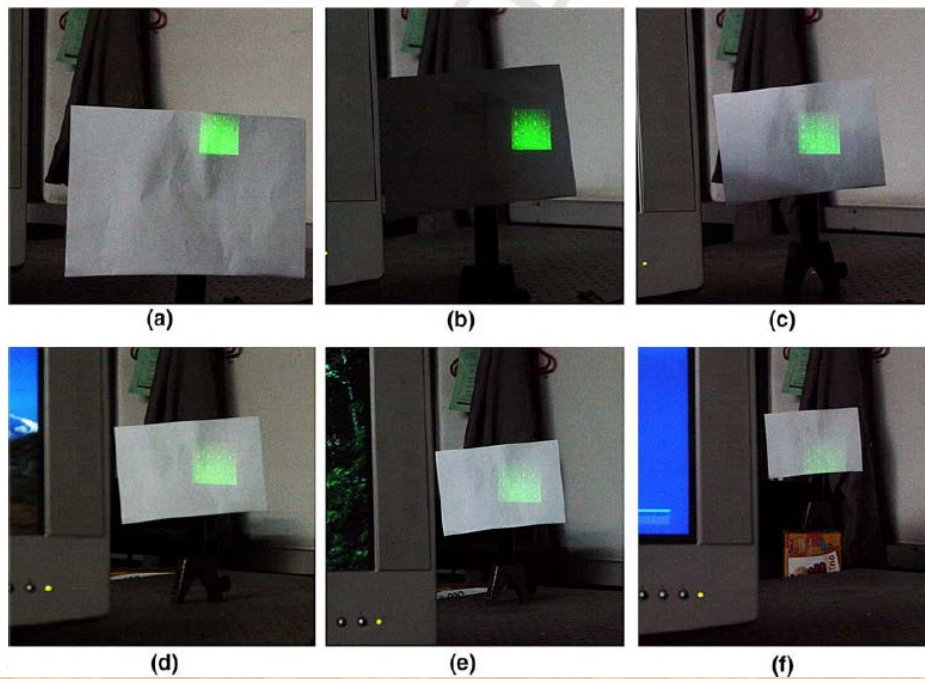
Speckles projection Z-varied distribution



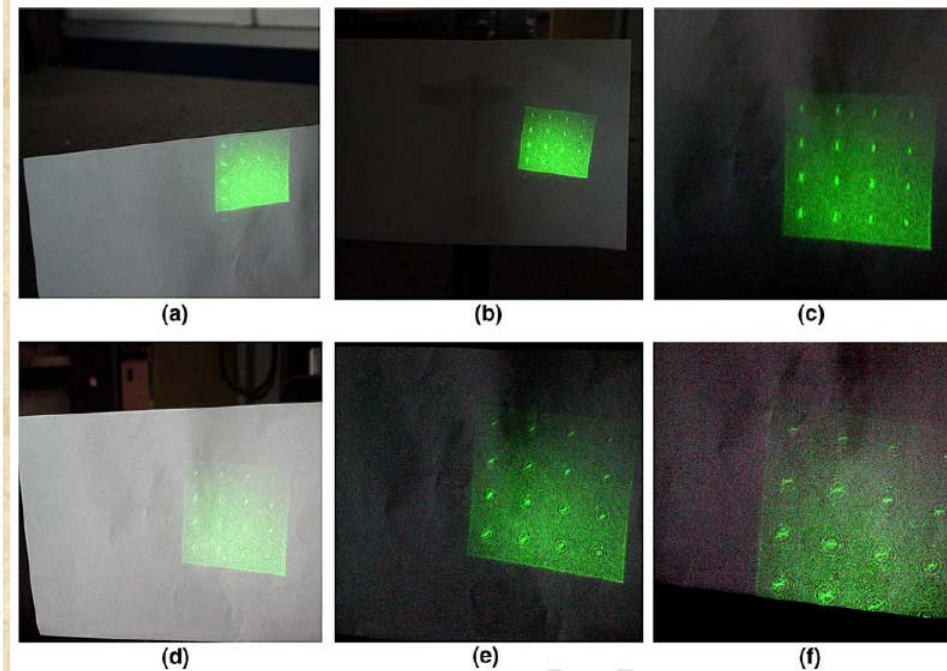
Projection of Z-varied random speckles distribution.



The patterns that were chosen to irradiate on planes at range: (a) 0.5, (b) 0.6, (c) 0.7, (d) 0.8, (e) 0.9, and (f) 1 m from the light source.



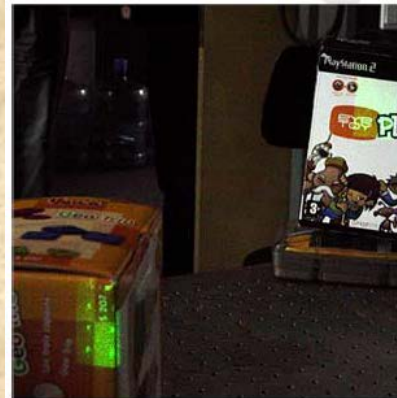
Images capturing the different patterns irradiating on planes (white paper) at range: (a) 0.5, (b) 0.6, (c) 0.7, (d) 0.8, (e) 0.9, and (f) 1 m from the light source. Note that the plane in image (b) seems to be darker due to the shadow falling from the computer screen placed on the left.



Enlargements of images (a)–(f) from previous figure around the areas consisting of the irradiation patterns depicting the directions of the slits.



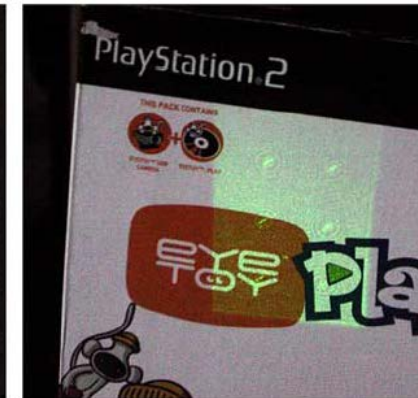
A semi-realistic scene where a mobile robot (a car) illuminates the scene using the proposed phase-only filter in order to detect obstacles. Two boxes are positioned in front of it, and it can be clearly seen that the pattern of the filter is split between both of them, where one half irradiate in a specific pattern and the other half irradiates in a different pattern.



(a)



(b)



(c)

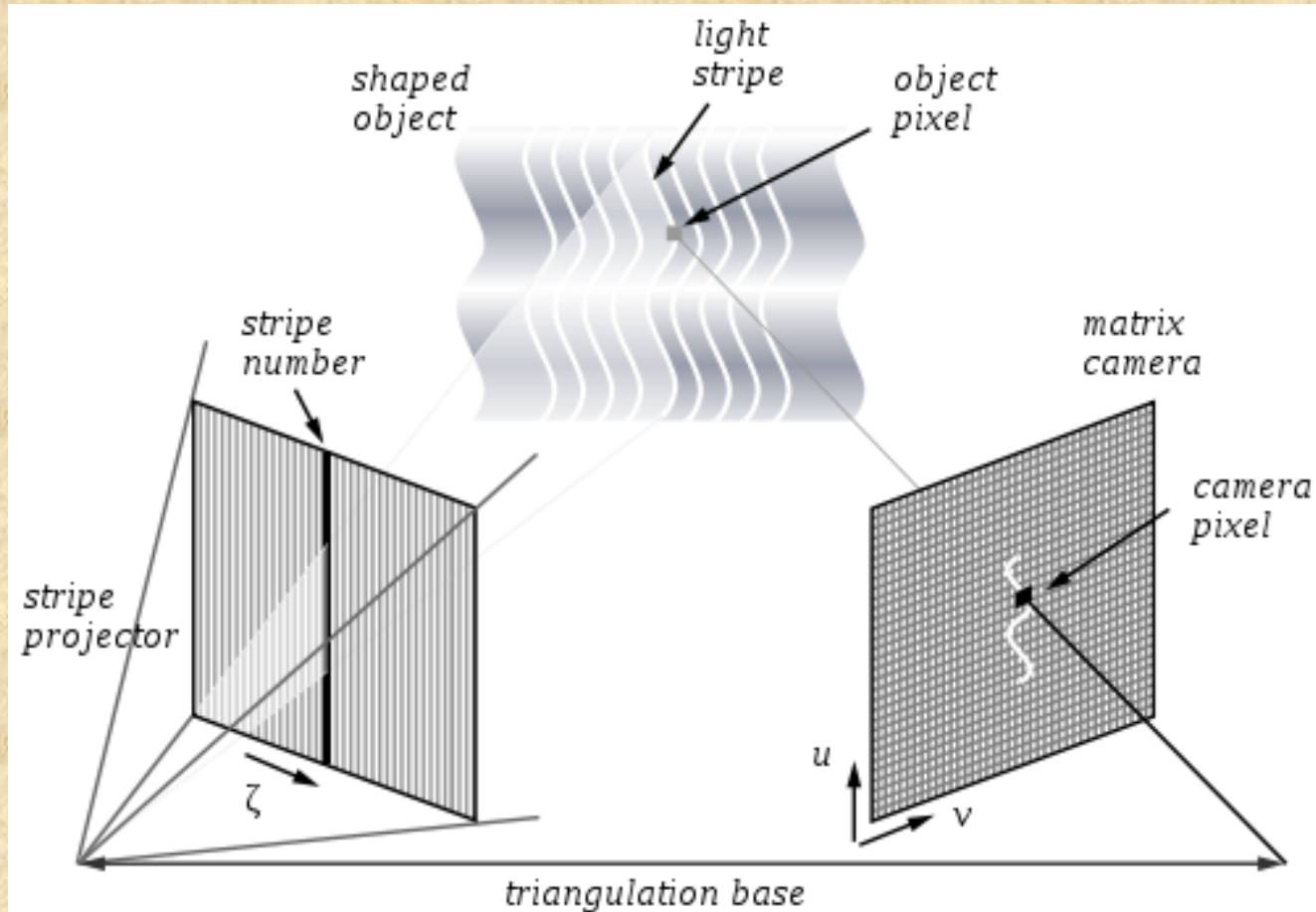
A closer observation of the scene demonstrated in the previous figure : (a) depicts both obstacles, while (b) and (c) depict even closer each obstacle.



The steps taken in order to automatically classify the pattern direction. (a) The image is aligned horizontally and its color is normalized. (b) A threshold is applied. (c) The slit pattern that gives maximum correlation response.

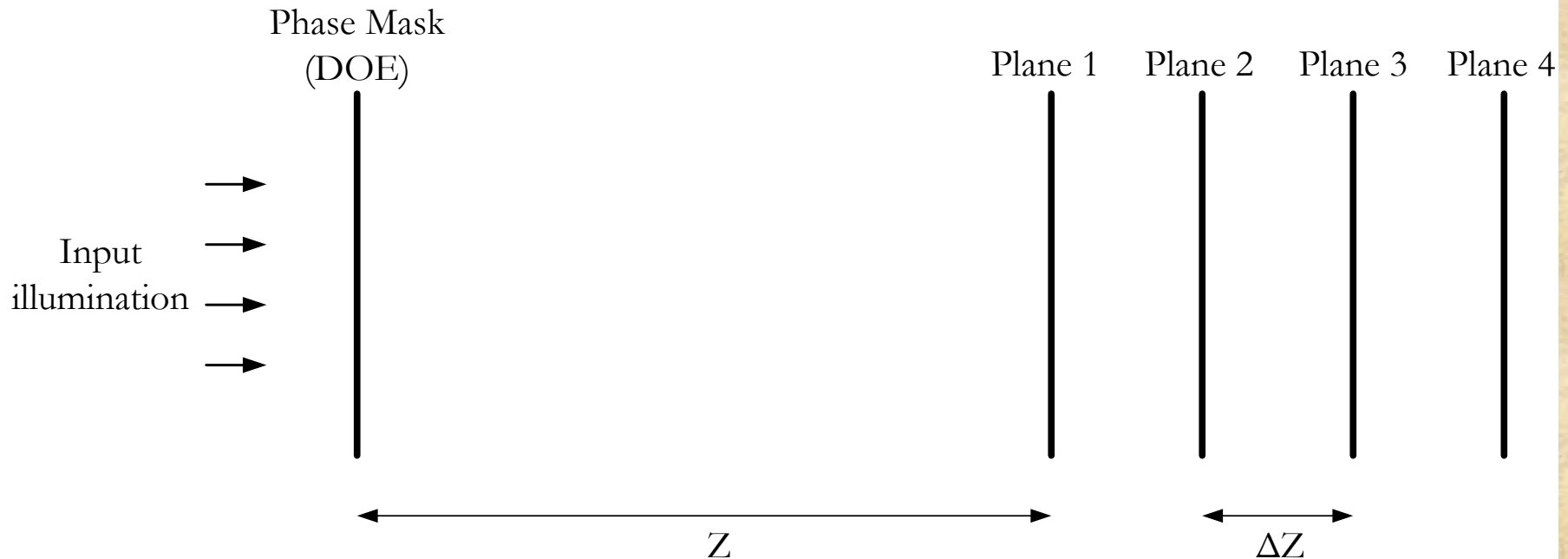
Outline

- Introduction
- Review of new approaches
- Correlation based 3D estimation
- Conclusions



Patterns projection setup has the same axial resolution limit as in conventional triangulation setups.

Schematic configuration



3-D setup of on-axis axially varying illumination. ΔZ designates the axial separation between two beam shaped planes.

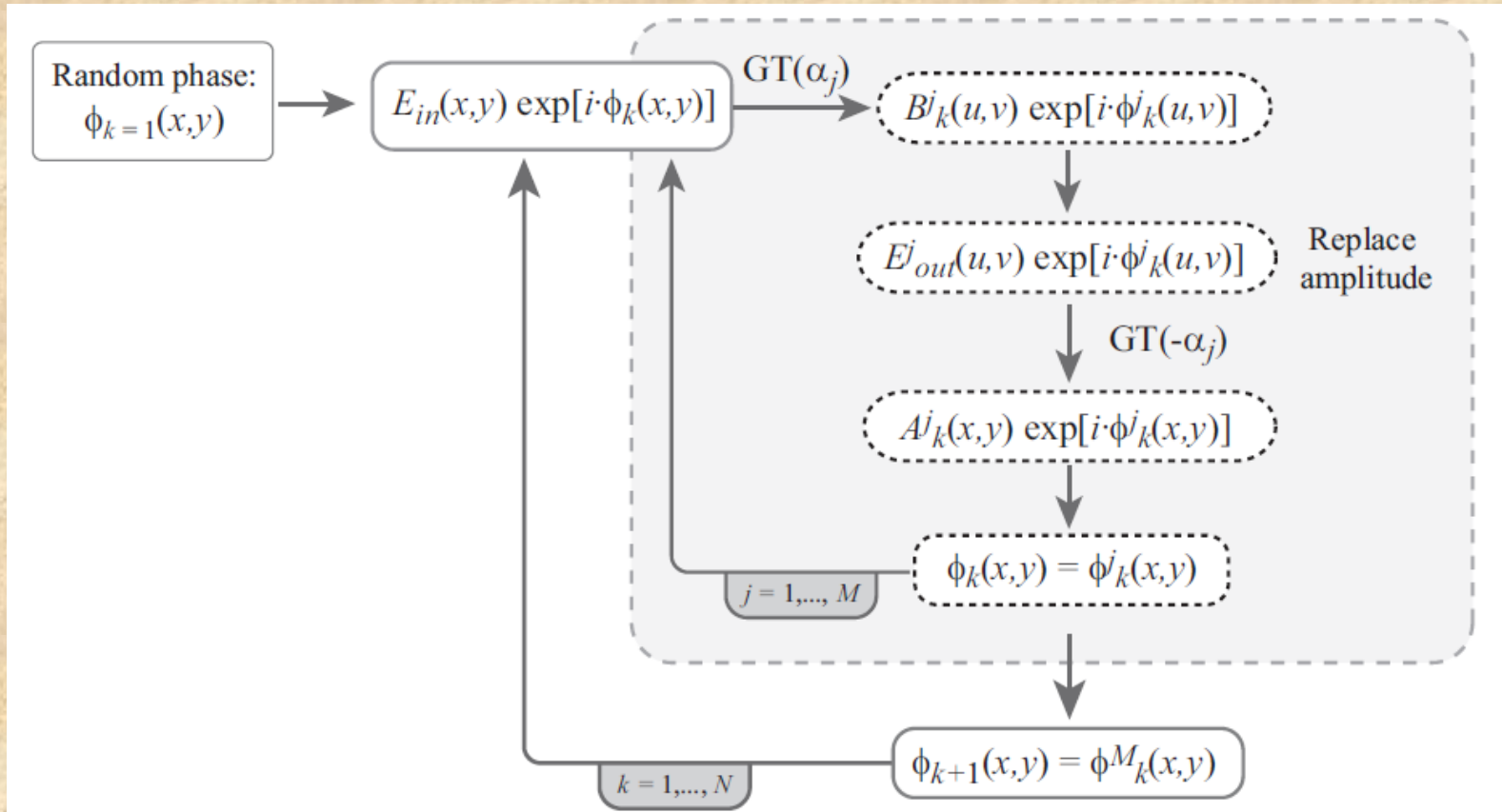
Existing Disadvantages:

- The triangulation scheme has axial resolution proportional to the angle between the projector and the camera.
- For Z-varied patterns projection, only limited number of distributions is feasible for realization.

Description:

- Designing phase element realizing N, Z-varied distributions via iterative numerical approach.
- Projection of the Z-varied patterns.
- Obtaining more than N axial discrimination planes by applying correlation based numerical computation over the back reflected distribution.
- Improving the ranging or the 3D resolution by one order of magnitude.
- Combining Z-varied projection with triangulation will further improve axial accuracy.

Iterative beam shaping design



N is the number of iteration cycles and M is the number of constrain planes. Here we use gyrator transform instead of Fresnel transform.

Correlation operation:

$$Corr_{A,B}(x, y) = \iint A(x', y') B^*(x' - x, y' - y) dx' dy'$$

The 3 measured parameters are defined as:

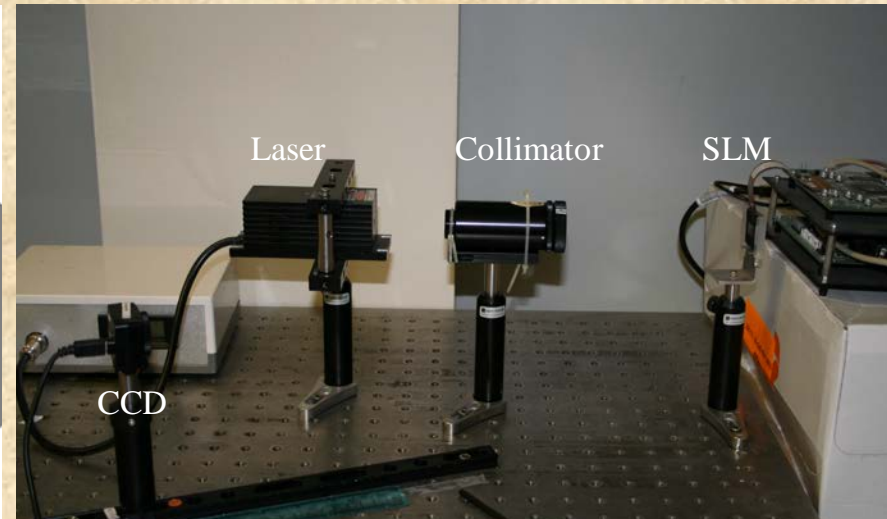
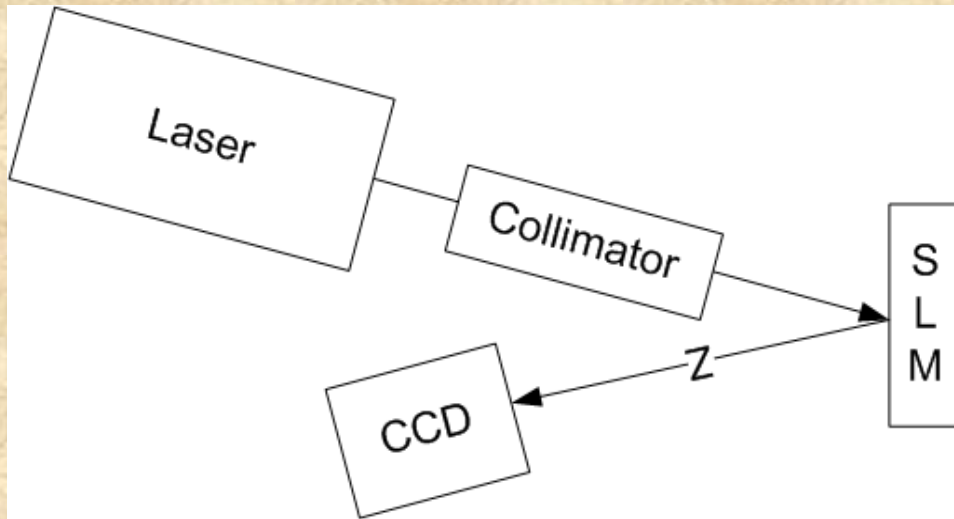
1. $ratio = \max \{Corr_{I,E_n}(x, y)\} / \max \{Corr_{I,E_{n+1}}(x, y)\}$
2. $SNR1 = \max \{Corr_{I,E_n}(x, y)\} / \text{mean} \{Corr_{I,E_n}(x, y) \mid x, y \notin \max \{Corr_{I,E_n}(x, y)\}\}$
3. $SNR2 = \max \{Corr_{I,E_{n+1}}(x, y)\} / \text{mean} \{Corr_{I,E_{n+1}}(x, y) \mid x, y \notin \max \{Corr_{I,E_{n+1}}(x, y)\}\}$

$I(x,y)$ is the reflected intensity image, $E_n(x,y)$ and $E_{n+1}(x,y)$ are the two sequential planes between which we aim to perform the interpolation.

Description:

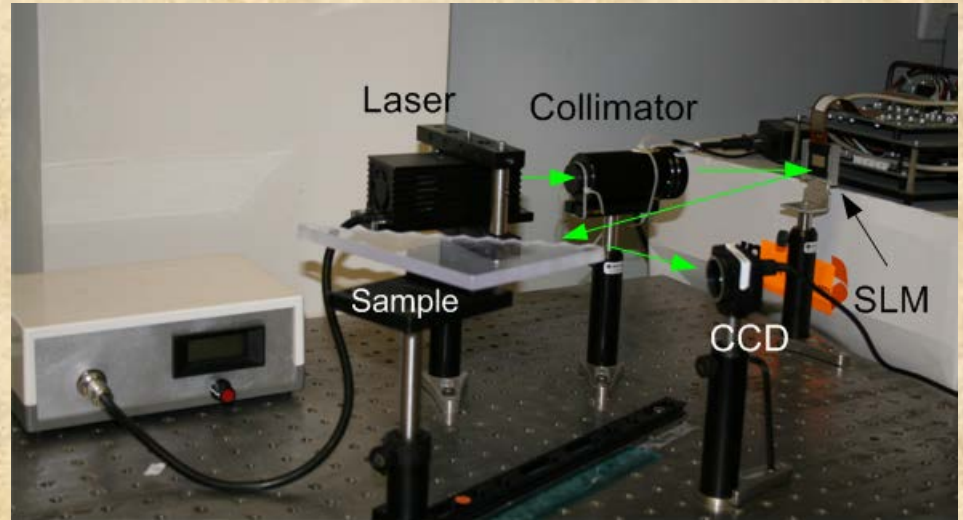
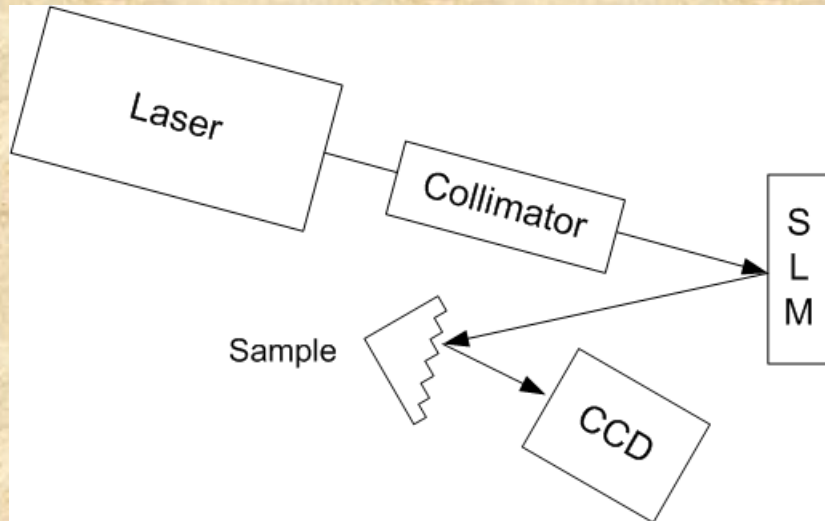
- Eq. 1 receives maximal value at axial position Z_n where we planed to receive the pattern $E_n(x,y)$, minimal value at position Z_{n+1} where we planed to receive $E_{n+1}(x,y)$ and values close to one at the middle range between these two planes.
- $\text{mean}\{\}$ is the average operator taken on all (x,y) positions except the one holding the maximal value.

Experimental configuration



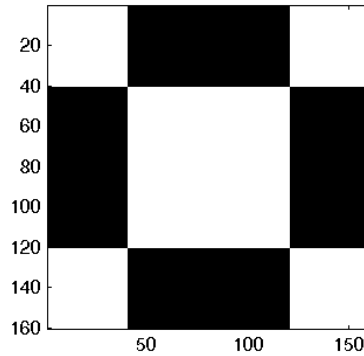
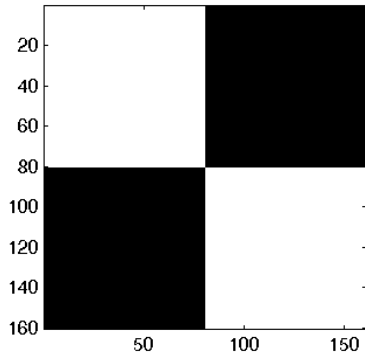
Experimental setup. (a). The SLM is illuminated by a collimated laser beam and the output intensity is captured by a CCD for different axial distances of Z . Note that by using a transparent instead of reflective SLM, object to be located would be placed after the SLM. (b). Image of the experimental setup.

Experimental configuration

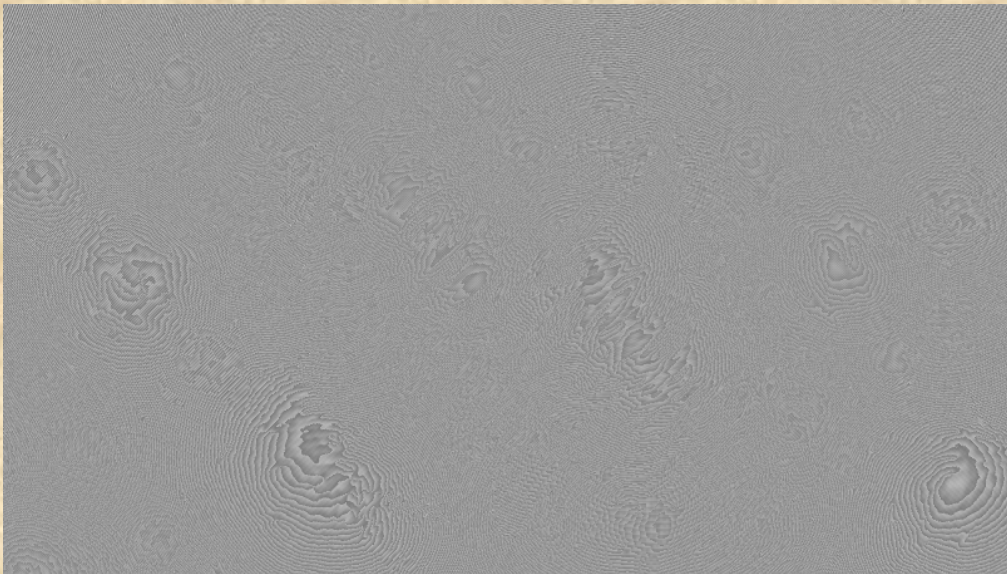


Experimental setup. (a). The SLM is illuminated by a collimated laser beam and the output intensity is captured by a CCD for different axial distances of Z . Note that by using a transparent instead of reflective SLM, object to be located would be placed after the SLM. (b). Image of the experimental setup.

Experimental results

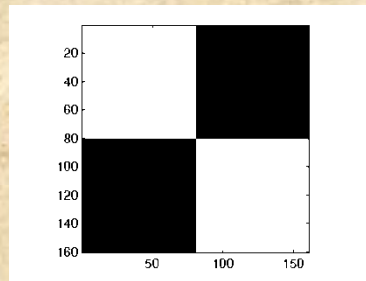
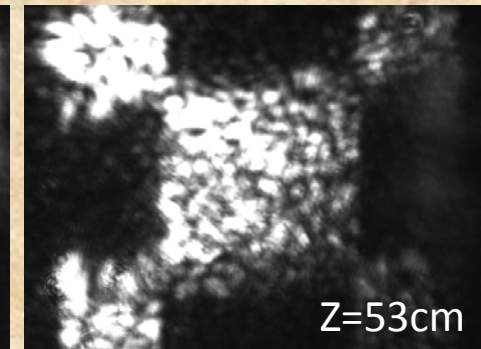
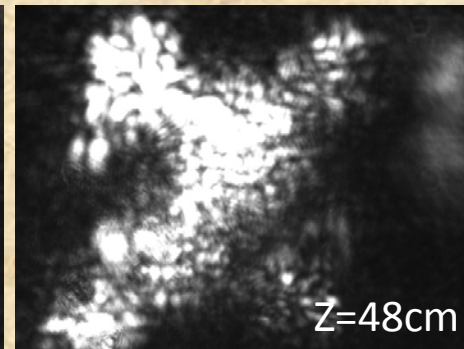
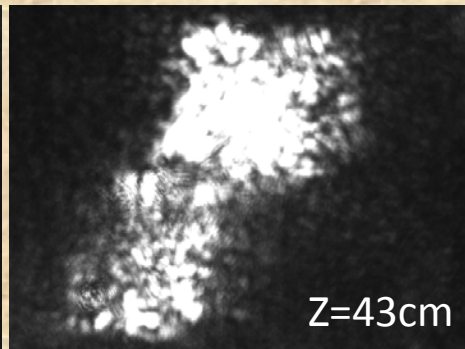
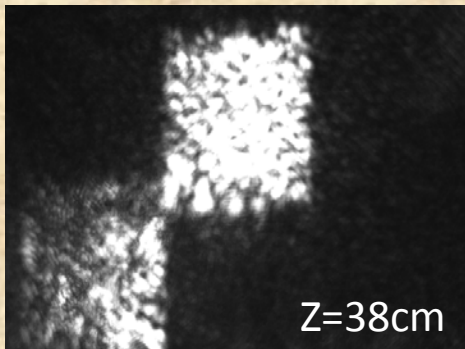


Desired illumination patterns. The images match the positions (a). $Z=40\text{cm}$ and (b). $Z=52\text{cm}$.

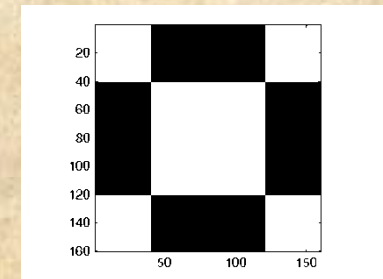


Phase element implemented via an SLM. The intensity of each of the 1920×1080 pixels is translated to a phase in the proper (x,y) location of the SLM.

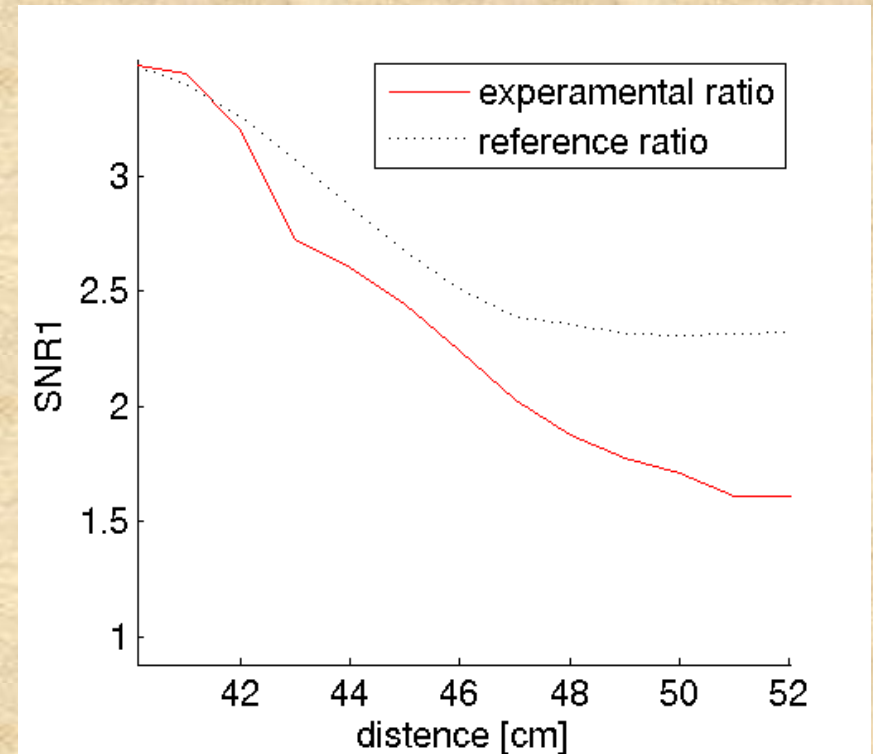
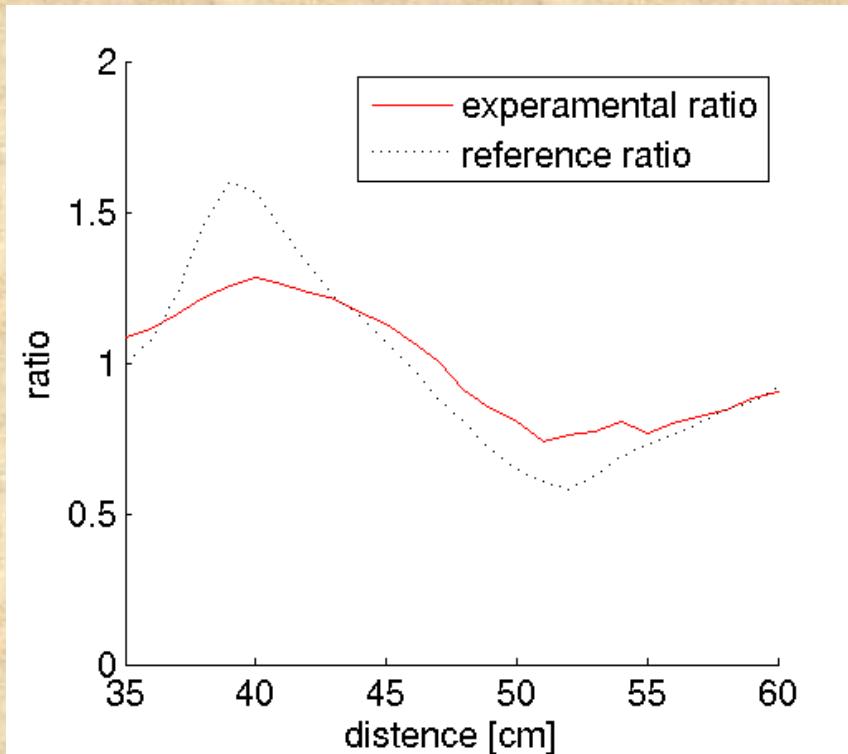
The experimental beam shaped distributions obtained along various axial positions.



Z

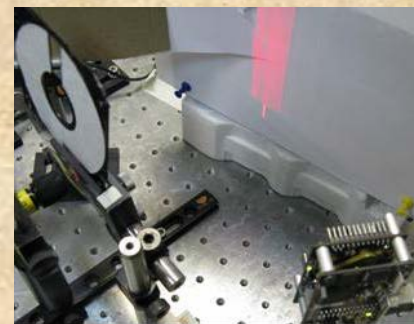


Experimental results

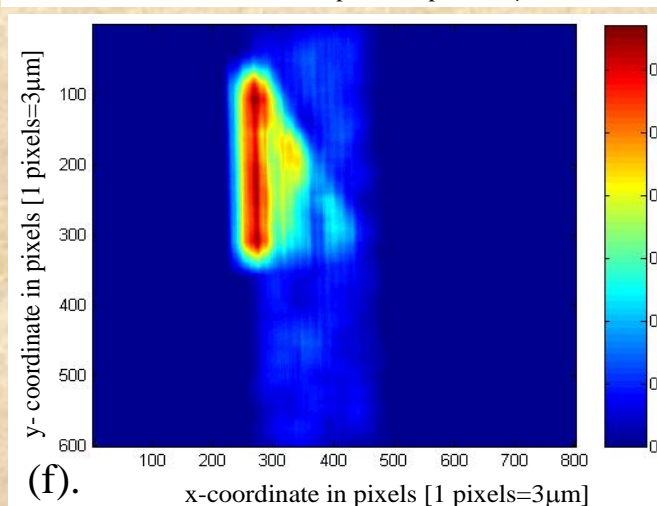
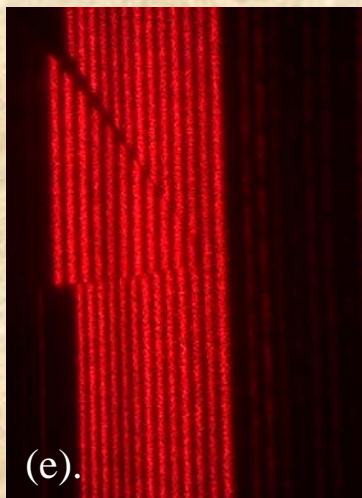
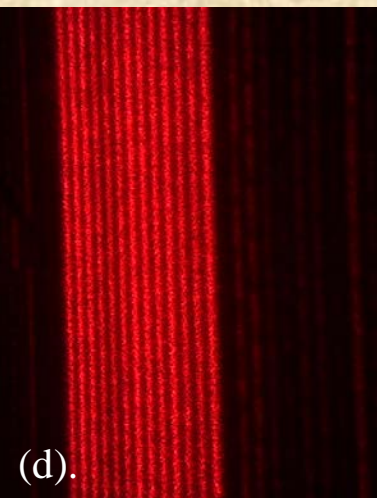
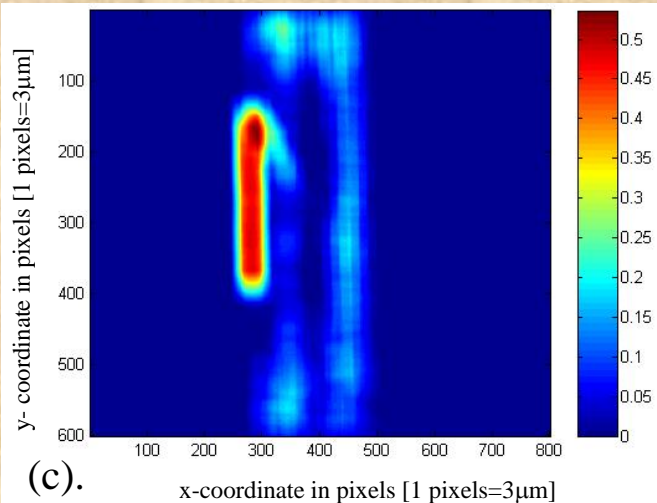
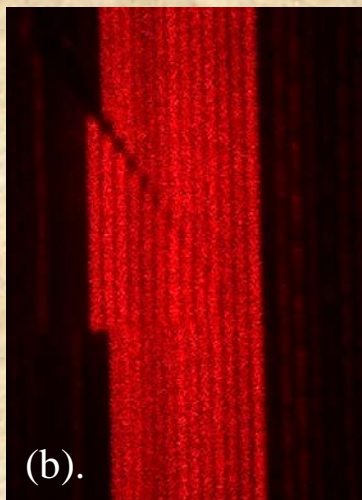
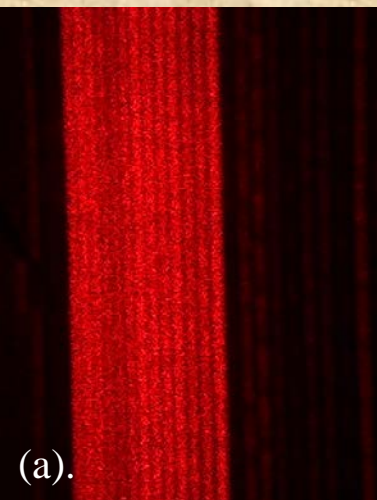


Interpolation parameters of experimental (red solid line) and simulation reference (black dotted line). (a). The maxima correlation peak ratio denoted ratio and (b). the first maximum to minimum ratio denoted SNR1. In this case, there is no need for the third parameter.

Extended depth of focus



- (a). The imaged grating without EDOF and without the inspected object. (b). The imaged grating without EDOF and with the inspected object. (c). 3-D reconstruction for the case of without EDOF. (d). The imaged grating with EDOF and without the inspected object. (e). The imaged grating with EDOF and with the inspected object. (f). 3-D reconstruction with EDOF.



Outline

- Introduction
- Review of new approaches
- Correlation based 3D estimation
- Conclusions

Conclusions

- Projection based techniques for ranging and 3D estimation were demonstrated.
- Correlation based algorithm for improved ranging/3D estimation was introduced.
- More than one order of improvement in the range estimation accuracy was experimentally demonstrated.

Thank you

